life

MDPI

Article

Maize Growth, Soil Properties and Microbial Communities Across Biochar Application Rates in Saline–Alkali Soil

Chi Zhang [1], Yu Miao [1], Fangze Li [1], Ge Zhang [1], Qiwei Sun [1], Tianci Hua [1], Zhikun Pang [1], Xingjie Lin [1,2,*] and Rui Li [1,3,4,*]

[1] Institute of Environment Engineering, BGRIMM Technology Group, Beijing 100160, China; zhangchiustb@foxmail.com (C.Z.); 491637611@163.com (Y.M.); lfze2016@163.com (F.L.); zhanggling@163.com (G.Z.); b20200050@xs.ustb.edu.cn (Q.S.); htc0101@163.com (T.H.); pzk728@163.com (Z.P.)
[2] School of Energy and Environmental Engineering, University of Science and Technology Beijing, Beijing 100083, China
[3] Research Center for Eco-Environmental Sciences, Chinese Academy of Sciences, Beijing 100085, China
[4] University of Chinese Academy of Sciences, Beijing 100049, China
* Correspondence: xingjielin@sina.com (X.L.); lirui18@mails.ucas.edu.cn (R.L.)

Abstract

Biochar adds carbon and mineral ash to soil, while crop responses can differ among application rates. We compared 0.5%, 1% and 2% maize-straw biochar in a greenhouse experiment with five blocks, comprising 15 planted amended pots and five control (CK) soil pots that contained no plants. Plant measurements and paired non-rhizosphere (NR) and rhizosphere (R) soil were obtained from the amended pots; 16S rRNA and ITS2 amplicons characterized soil bacterial and fungal communities. CK was sampled over 0–20 cm, whereas amended NR soil was sampled at 15–20 cm. The CK–amended differences are therefore descriptive; treatment inference uses the amended rates. The mean grain yield was highest at 1% (55.6 g plant^{-1}), but the 1–2% difference was uncertain (7.32 g plant^{-1}; Bonferroni 95% CI −3.52 to 18.16; BH q = 0.114). The photosynthetic rate was 3.16 μmol m^{-2} s^{-1} higher at 1% (Bonferroni 95% CI −0.92 to 7.24; BH q = 0.0475). At 2%, NR total organic carbon exceeded CK by 12.31 g kg^{-1}, including added biochar carbon. The bacterial and fungal composition differed among amended rates after adjustment for block (R^2 = 0.299 and 0.653; both p = 0.00077). Neither environmental db-RDA model passed corrections across the two markers, and none of 33 soil–plant associations survived correction after treatment and block were accounted for. These differences do not establish a field optimum or microbial mediation.

Keywords: biochar; saline–alkali soil; maize; rhizosphere; bacteria; fungi; application rate

Academic Editor: Pabulo Henrique Rampelotto

Received: 30 August 2026
Revised: 19 October 2026
Accepted: 21 October 2026
Published: 23 October 2026

Copyright: © 2026 by the author. Licensee MDPI, Basel, Switzerland. This article is an open access article distributed under the terms and conditions of the Creative Commons Attribution (CC BY) license.

1. Introduction

Saline–alkali soils impose osmotic, ionic and alkaline stresses on plants and soil microorganisms [1–3]. An estimate cited in a 2017 reply by China's National Development and Reform Commission placed saline–alkali land at approximately 100 million ha, including non-cultivated land [4]. A remote-sensing study mapped about 2051 km^2 of salt-affected land within its Yellow River Delta study area in 2020 [5]. These estimates describe different geographical and land-use scopes. Biochar may change salt stress, water retention and nutrient availability, although responses depend on the soil, feedstock and

application rate [6,7]. Experiments have also reported different plant and rhizosphere responses among crops and biochar materials [8,9]. Comparisons among application rates must distinguish the carbon and minerals added with biochar from changes in plant growth and soil biological activity.

Biochar responses vary with soil properties, feedstock and application rates [6,7,10]. Increases in soil carbon or microbial biomass do not consistently coincide with increases in microbial diversity or plant growth [7,10,11]. Bacterial and fungal communities can also respond differently in salt-affected soils [12,13]. We asked whether the rate producing the greatest maize growth differed from the rate producing the highest measured soil carbon and nutrient concentrations, and whether microbial composition and biomass differed between rhizosphere and non-rhizosphere soil within amended pots. These questions were evaluated through amended-rate and paired-zone comparisons; a split-plot test was also used to estimate the treatment-by-zone interaction.

Roots alter local conditions and influence which microorganisms occur near the root surface [14]. Taxon filtering, compositional data and small sample sizes can affect inferred relationships [15–23]. Amplicon profiles describe composition, whereas microbial biomass, respiration and enzyme assays measure different biological properties. Neither shared treatment responses nor correlation networks alone establish a microbial cause of plant growth.

This study extends an earlier report from the same experiment by examining maize growth, photosynthesis and ion balance alongside enzyme activities and microbial biomass. The related paper focused on nitrogen status, dissolved organic matter and their microbial associations [24]. Soil samples and amplicon profiles are shared, and community composition is reanalyzed here rather than presented as an independent dataset. Our additional question is whether the plant responses coincide with measured soil and microbial responses after accounting for treatment and block. The experiment comprised 15 amended pots and five CK soil pots without plants; CK reported bulk (non-rhizosphere) soil only, and no CK rhizosphere or CK plant data were available. Plant–soil associations therefore only use the 15 amended pots with matched measurements.

2. Materials and Methods

2.1. Pot Experiment and Materials

The experiment was conducted in a greenhouse at an agricultural base in Xiong'an New Area, Hebei, China (38°53′34″ N, 116°1′5″ E), using coastal alluvial saline–alkali soil from the Yellow River Delta. The initial soil pH was 8.83 and electrical conductivity (EC) was 2.41 dS m^{-1}. The extraction ratio for the initial EC measurement was not separately recorded; the harvest EC measurements used a 1:5 soil:water ratio. Soil texture and initial TOC, TN, available P, available K and ESP were not measured. Air-dried soil was passed through a 2 mm sieve. Each plastic pot contained 8 kg soil and had an internal diameter and height of 20 cm, drainage holes and a tray. Maize-straw biochar (BC) was mixed throughout the soil at 0, 0.5%, 1% or 2% (*w*/*w*), equivalent to 0, 40, 80 or 160 g per pot. The three nonzero rates ranged from 5 to 20 g kg^{-1} soil to compare responses across application rates without estimating a continuous optimum. General chemical reagents were of analytical grade (AR) and were supplied by Thermo Fisher Scientific (Waltham, MA, USA).

The experiment comprised five blocks and 20 distinct pots. Each block contained one pot at each biochar rate (0.5%, 1% and 2%) and one CK soil pot without plants. The 15 amended pots reported both plant and soil measurements; maize was sown in the five CK pots, but no plants grew. CK pots provided bulk soil and amplicon samples only. Treatment positions were assigned within blocks by random allocation, and pot positions were randomized again each week to reduce persistent light and temperature effects. Three seeds of maize (*Zea mays* L. cv. Zhengdan 958) were sown 3 cm deep in each amended pot

on 11 April 2023. Multiple plants were retained in each amended pot, and plant number differed among treatments. Pots were maintained at 25 ± 3 °C under natural light. Light intensity and relative humidity were not recorded. Tap water was added by weighing pots to maintain a 60–70% water-holding capacity daily during the warmest period and every 2–3 days otherwise. Irrigation-water EC and ion composition were not measured. No mineral fertilizer, insecticide or fungicide was applied. All pots were harvested on 10 July 2023, 90 days after sowing and approximately one month after tasseling. The investigators judged the plants ready for harvest from their apparent maturity; black-layer formation and grain moisture were not used as criteria. This harvest timing does not independently establish physiological grain maturity. There were therefore 20 distinct pots: 15 amended and five CK soil pots without plants; the dataset contained 35 soil profiles (20 NR + 15 R). No CK plant data were available.

Maize straw was air-dried and ground to <2 mm before pyrolysis in a programmable muffle furnace (SX2-4-10; Shanghai Shangdao Instrument Manufacturing Co., Ltd., Shanghai, China) under limited oxygen at 500 °C, with a heating rate of 10 °C min^{-1} and a residence time of 2 h; the furnace was purged with N_2 before heating [24]. Biochar yield was 32.5%. The characterization record gives a TOC of 63.14%, total carbon of 63.32%, inorganic carbon of 0.18% and TN of 0.34%. Its pH was 9.52, EC was 3.87 dS m^{-1}, BET surface area was 24.8 m^2 g^{-1} and total pore volume was 0.042 cm^3 g^{-1}. H/C and O/C ratios were 0.55 and 0.22, respectively; ash content was 16.1%, CEC was 28.5 cmol kg^{-1} and pH at the point of zero charge was 8.2. Characterization procedures and the distinction between the TOC and proximate fixed carbon are given in Section S10. An independent analytical certificate was not available for these characterization results.

At harvest, loose soil was removed by gentle shaking of the root systems, and soil still adhering to the roots was detached with a soft brush. Approximately 500 g of this rhizosphere soil was collected from multiple plants within each amended pot to form one R sample. Non-rhizosphere soil was collected using a sterile soil corer at 15–20 cm depth from locations that were more than 1 cm away from visible roots. CK was sampled as bulk soil over 0–20 cm; amended NR soil was taken at 15–20 cm. Soil samples were sieved, and subsamples were stored at −80 °C for DNA extraction, at 4 °C for fresh-soil assays, or air-dried for physicochemical measurements. Each amended pot provided one R and one NR sample, whereas CK provided one NR sample per pot. The dataset therefore contained 35 soil profiles from 20 pots. The pot-level design and sample audit are provided in Table S15. NR and R denote non-rhizosphere and rhizosphere samples throughout the text and figures; the corresponding original sample codes are F and G.

The soil samples and amplicon profiles overlap with those used in the companion study [24]. The present analyses use the 15 amended pots and five CK soil pots without plants; no CK plant data are used. The two reports are not independent biological replicates.

2.2. Soil Physicochemical Properties

Harvest soil pH and EC were measured in 1:5 soil:water extracts using a PHS-3C pH meter and a DDS-307A conductivity meter (both from Shanghai INESA Scientific Instrument Co., Ltd., Shanghai, China), respectively [25–27]. Gravimetric soil water content was determined after oven-drying at 105 °C for 24 h and expressed as water mass divided by dry-soil mass. Total soluble salts were quantified gravimetrically from dried soil–water extracts according to NY/T 1121.16-2006 [28]. Available P was determined by sodium bicarbonate extraction followed by molybdenum–antimony spectrophotometry (HJ 704-2014) [29,30]. Available K was measured by ammonium acetate extraction and flame photometry using an FP640 flame photometer (Shanghai INESA Analytical Instrument Co., Ltd., Shanghai, China; NY/T 889-2004) [31]. Organic matter was estimated by loss on

ignition at 600 ± 20 °C for 3 h, applying the HJ 761-2015 procedure to these soil samples [32]. This standard applies to solid waste, not specifically to soil. The resulting variable is treated as an LOI-derived proxy because inorganic mass loss can affect the estimate [33]. For TOC and TN, air-dried soil was ground and passed through a 100-mesh sieve, then analyzed with a vario MACRO cube elemental analyzer (Elementar Analysensysteme, Langenselbold, Germany). TOC aliquots were placed in silver boats and fumigated with HCl at 60 °C for 24–48 h to remove inorganic carbon; they were thoroughly dried to remove residual acid before combustion analysis. TN was measured on separate, unacidified soil aliquots to avoid N loss during pretreatment. TOC was measured independently, not calculated from TC minus IC or determined by dichromate oxidation. Original instrument and calibration files were unavailable for independent numerical verification.

NH_4^+-N was measured in 2 mol L^{-1} KCl extracts of fresh soil by indophenol-blue colorimetry at 630 nm, with reference to HJ 634-2012 [34] and the KCl concentration specified by the experimental record. For NO_3^--N, fresh soil and 2 mol L^{-1} KCl were combined at 1:5 (g:mL) and shaken for 2 h. After centrifugation and filtration, the extract was diluted tenfold and measured at 220 and 275 nm. Corrected absorbance was calculated as $\Delta A = A_{220} - 2A_{275}$ and quantified against a standard curve, using dual-wavelength UV spectrophotometry [35]. The mass conversion and its verification limits are given in Section S10. The total dissolved nitrogen in fresh-soil extracts was measured after alkaline persulfate digestion at 120–124 °C, applying HJ 636-2012 to the soil extract [36]. Dissolved organic nitrogen was calculated by subtracting measured NH_4^+-N and NO_3^--N from the total dissolved nitrogen. Water-soluble Na^+, Ca^{2+}, Mg^{2+} and K^+ were measured in 1:5 water extracts by ICP-OES (Vista Pro; Varian Australia Pty Ltd., Mulgrave, Victoria, Australia), and Cl^- and SO_4^{2-} by ion chromatography (Dionex Aquion; Thermo Fisher Scientific, Sunnyvale, CA, USA). Soil CEC was determined by hexamminecobalt(III) chloride extraction and spectrophotometry, using the exchange-depletion principle described in HJ 889-2017 [37]. Hexamminecobalt ions displaced exchangeable cations, and their concentrations before and after extraction were measured with a UV-1900i spectrophotometer (Shimadzu, Kyoto, Japan); the CEC was calculated from the decrease in solution concentration. For exchangeable Na, soil was first washed with 60–70% ethanol to remove soluble Na salts, then extracted with ammonium acetate and analyzed by ICP-OES. ESP was calculated as exchangeable Na divided by CEC in matching charge units, multiplied by 100. Carbon, nitrogen fractions, water-soluble ions and available K are reported on a dry-soil basis [25,26].

The five CK-NR samples had a mean NO_3^--N of 383.49 mg kg^{-1} and TN of 0.67506 g kg^{-1}, giving a NO_3^--N:TN ratio of 56.81% after unit conversion. KCl-extractable nitrate is an operationally defined soil measurement. Original absorbance and calibration records were unavailable; the high nitrate fraction of TN therefore remained unverified and was not used to infer N turnover.

2.3. Plant Measurements

Plant growth and yield traits included plant height, stem diameter, shoot dry weight, root dry weight, 100-grain weight and grain yield. Measurements were averaged within each amended pot, giving one observation per pot and 15 independent pot-level means. Shoot and root dry weights and grain yield were expressed per plant, not as whole-pot totals. Shoot dry weight comprised stems and leaves and excluded ears and kernels. Shoot and root dry weights were determined after oven-drying at 72 °C for 24 h. Grain was air-dried before weighing; grain yield and 100-grain weight were not adjusted to a standard moisture content. Gas exchange was measured on healthy, mature ear leaves with an LI-6800 portable photosynthesis system (LI-COR, Lincoln, NE, USA) between 9:00 and 11:00 on the seventh day after tasseling. Chamber PAR was 1200 μmol m^{-2} s^{-1} with a 9:1 red:blue

light ratio; reference CO_2 was 420 μmol mol^{-1}, flow was 500 μmol s^{-1} and fan speed was 10,000 rpm. Humidity was adjusted to maintain the leaf-to-air vapor-pressure deficit at 1.0–1.5 kPa. After stabilization, the infrared gas analyzers were matched, and the net photosynthetic rate (Pn), stomatal conductance (Gs), transpiration rate (Tr) and intercellular CO_2 concentration (Ci) were recorded, with correction for the actual enclosed leaf area. The plant dataset also reports water-use efficiency (WUE). Plant measurements, including gas exchange, were summarized as within-pot means. No CK plant measurements were available.

For plant-ion measurements, dried whole-plant material was ground, ball-milled and passed through a 200-mesh sieve. A 0.5 g portion was microwave-digested for 1 h with 6 mL HNO_3, 3 mL HCl and 2 mL HF. A further 2 mL HNO_3, 1 mL HF and 1 mL $HClO_4$ were added, followed by temperature-controlled acid removal for approximately 3 h. The digest was made up to 25 mL with 1% HNO_3, allowed to stand for 1 h and filtered through a 0.45 μm membrane. Na, K, Ca and Mg were measured by ICP-OES (Vista Pro; Varian Australia Pty Ltd., Mulgrave, Victoria, Australia), and plant K^+/Na^+ was calculated from the measured concentrations. This acid-digestion procedure was adapted from HJ 832-2017, whose stated scope was soil and sediments [38]. The ion assay used whole plants; the resulting concentrations and K^+/Na^+ ratio were not organ-specific.

Chlorophyll was extracted from 2 g of fresh leaf tissue ground with quartz sand, calcium carbonate powder and ethanol. The extract was filtered into a brown volumetric flask, made up with ethanol, and measured at 665 and 649 nm against an ethanol blank. Chlorophyll a and b were expressed as mg g^{-1} fresh weight (FW), using an ethanol-extraction spectrophotometric approach [39]. Chlorophyll, carotenoid and SPAD values were excluded from the plant performance index and treatment comparisons because the extraction coefficients and assay details were not recorded.

2.4. Enzyme Activities and Measured Microbial Physiology

Soil urease, alkaline phosphatase, catalase, cellulase and sucrase activities were determined with commercial soil enzyme kits (Solarbio, Beijing, China). For urease, alkaline phosphatase, catalase, cellulase and sucrase, respectively, 1 U g^{-1} denotes 1 μg NH_3-N released, 1 nmol phenol released, 1 mmol H_2O_2 decomposed, 1 mg glucose released or 1 mg reducing sugar released per gram of soil per day; catalase uses air-dried soil. These day-based definitions are distinct from the actual incubation durations. Temperatures, incubation times and wavelengths are listed in Section S10 and Table S3. Urease activity was determined by ammonium-release colorimetry [40]. Alkaline phosphatase activity was measured by phenol-release colorimetry [41]. Catalase activity was determined from the decrease in H_2O_2 absorbance at 240 nm; permanganate titration was not used. Cellulase and sucrase activities were determined by glucose and reducing-sugar colorimetry, respectively [42,43]. Their U g^{-1} values use different biochemical definitions and are not comparable as a common unit; original calibration and time-normalization worksheets were unavailable, so the reported magnitudes remained unverified.

MBC and MBN were determined by chloroform fumigation–extraction, using extraction-efficiency factors K_EC = 0.45 and K_EN = 0.54, respectively [44–46]. The measured ranges were 117.6–803.0 mg kg^{-1} for MBC and 17.5–104.3 mg kg^{-1} for MBN. The metabolic quotient qCO_2 was calculated as basal respiration divided by MBC, expressed as mg CO_2 g^{-1} MBC h^{-1} [47]. The incubation conditions for basal respiration were not recorded. qCO_2 is therefore reported as a descriptive variable and was not used as a predictor or in the composite indices.

2.5. DNA Extraction, Sequencing and zOTU Analysis

Total soil DNA was extracted from 0.5 g soil taken from subsamples stored at −80 °C using the E.Z.N.A. Soil DNA Kit (D5625-02; Omega Bio-tek, Norcross, GA, USA) [24]. Samples were bead-beaten for 4 min, treated with P2 buffer and cHTR reagent, and purified on HiBind columns. Columns were washed once with HBC buffer and twice with DNA Wash Buffer. DNA was eluted with 70 μL prewarmed buffer, yielding approximately 65 μL extract. DNA concentration and quality were assessed by Qubit 3.0 fluorometry and NanoDrop spectrophotometry (Thermo Fisher Scientific, Waltham, MA, USA) and 1.2% agarose gel electrophoresis. The bacterial 16S rRNA V3–V4 region was amplified with 338F/806R [48], and fungal ITS2 with ITS3/ITS4 [49]. A two-step PCR introduced Nextera-compatible dual indexes and independent 12 bp sample barcodes. Two extraction blanks had DNA concentrations below 0.1 ng μL^{-1} and no qPCR amplification; they were not sequenced. Library-PCR no-template controls showed no detectable bands. Meige Gene (Guangzhou, China) sequenced 35 libraries per marker on an Illumina NovaSeq 6000 platform (Illumina, San Diego, CA, USA) with paired-end 250 bp reads. The sequencing project is registered in the Genome Sequence Archive under BioProject accession PRJCA066142.

Marker amplification used TransStart FastPfu DNA Polymerase (TransGen Biotech, Beijing, China) in 20 μL reactions containing 4 μL of 5× FastPfu buffer, 2 μL of dNTPs (2.5 mmol L^{-1}), 0.8 μL of each primer (5 μmol L^{-1}), 0.4 μL of polymerase, 10 ng of template DNA and water to volume. For 16S V3–V4, the program was 95 °C for 3 min; 27 cycles of 95 °C for 30 s, 55 °C for 30 s and 72 °C for 45 s; and 72 °C for 10 min. For ITS2, it was 95 °C for 3 min; 35 cycles of 95 °C for 30 s, 55 °C for 30 s and 72 °C for 30 s; and 72 °C for 10 min. Each sample was amplified in three technical replicates. Products were checked by 2% agarose gel electrophoresis, purified with the AxyPrep DNA Gel Extraction Kit (Axygen Biosciences, Union City, CA, USA), quantified fluorometrically and pooled at equimolar concentrations. These are the marker-amplification conditions; a separate complete indexing-PCR cycling record was not retained.

Paired-end reads were processed locally with VSEARCH [50] and USEARCH/UNOISE3 [51,52]. The retained analysis record identifies VSEARCH 2.31.0 and USEARCH 12.0. Merged reads used for zOTU discovery were filtered at a maximum expected error of 1.0 and a minimum length of 200 bp, with no ambiguous bases allowed. Full-length dereplication retained sequences observed at least twice, and UNOISE3 used a minimum abundance of eight reads. Read-abundance tables were generated by mapping per-sample merged-read inputs to the representative zOTUs at 97% sequence identity and combining the sample tables by zOTU identifier. For the 16S mapping inputs, the retained script applied a separate filter of a maximum expected error of 10.0 and minimum length of 50 bp. The corresponding ITS mapping-input filter settings were not retained in a separate execution script. The 97% assignment threshold does not represent exact-match sequence counting. The preserved single-sample tables reconcile exactly with the count tables used here; the analysis was not reconstructed end to end from raw FASTQ files (Section S9).

Taxonomy was assigned using the SINTAX algorithm [53] implemented in VSEARCH 2.31.0 at a confidence threshold of 0.8 using a SILVA 138 reference for bacteria [54] and a UNITE reference for fungi [55]. Phylum summaries used the confidence-filtered assignments, with unsupported phylum assignments grouped as unclassified. The exact reference FASTA files and their checksums were not retained, so the UNITE release and finer SILVA version could not be independently resolved. For the supplementary phylogenetic diagnostic, representative sequences were aligned with MAFFT 7.526 using --auto [56], and trees were inferred with VeryFastTree 4.0.5 using its nucleotide option, a Jukes–

Cantor model and a CAT approximation with 20 rate categories [57]. The fungal ITS2 tree was not used for ecological assembly inference.

Before the current composition analyses, 51 bacterial non-target features annotated as chloroplasts, mitochondria or Archaea were excluded. The filtered bacterial table contained 26,096 zOTUs and 4,196,710 reads, with 81,622–164,682 reads per profile (mean 119,906). The fungal table contained 1952 zOTUs and 4,894,848 reads, with 84,987–231,371 reads per profile (mean 139,853). Bray–Curtis distances were calculated from within-profile relative abundances without rarefaction. These are analysis-table depths, separate from raw FASTQ read pairs and the clean-read summaries. A complete raw-read-to-table reconstruction was not performed (Section S9).

2.6. Statistical Analysis

The pot was the experimental unit. Growth, biomass, yield and gas-exchange measurements entered the analysis as within-pot means; each plant-ion variable likewise had one observation per pot. Individual plants were not treated as independent replicates. Plant traits and amended-only NR soil and microbial measurements were analyzed with y ~ Treatment + Block (n = 15; residual df = 8). CK pots contained no plants and were sampled over 0–20 cm; their comparisons with amended NR soil were descriptive observed group differences from a separate 20-profile model, with no treatment attribution. Paired-zone models excluded CK and used y ~ Treatment × Zone + Block + (1 | Pot_ID), with 30 observations from 15 pots, fitted by restricted maximum likelihood using nlme::lme (nlme 3.1-169) [58]. Estimated marginal means and contrasts were calculated with emmeans 2.0.3 [59]. BH correction [60] was applied to the three amended-rate contrasts within each endpoint or the three rate-specific paired-zone contrasts. Rate-contrast intervals reported in the text are simultaneous Bonferroni 95% intervals across three contrasts; mean and paired-zone intervals are unadjusted 95% intervals. Bonferroni intervals and BH q values use different multiplicity procedures and need not give identical threshold decisions. To assess multiplicity across endpoints, Table S14 also reports BH adjustment across all 132 amended-rate contrasts; these analyses are exploratory, with no retrospectively designated confirmatory primary endpoint. The descriptive soil index subtracts the mean z-score of pH, EC, total salt, ESP, Na^+, Cl^- and SO_4^{2-} from the mean z-scores of TOC, TN, available P, available K and water content. Variables were standardized using the sample mean and SD across all 35 profiles. LOI-derived organic matter and CEC were excluded. The index includes added biochar carbon; it is a descriptive summary, not an independently validated measure of soil health.

Community analyses used Bray–Curtis dissimilarities, principal coordinate analysis (PCoA), PERMANOVA and multivariate dispersion tests (PERMDISP) [61–64]. Counts were converted to within-profile relative abundances without rarefaction. Amended-rate comparisons used the 15 amended NR profiles with distance ~ Block + Treatment and a marginal Treatment test (df = 2, 8). All 7775 non-identity permutations within the five blocks were enumerated. The paired interaction test used distance ~ Pot_ID + Zone + Treatment:Zone on 30 amended profiles, with 9999 within-pot permutations (seed 20261019). Pot_ID absorbed between-pot variation, including treatment and block; the interaction was tested after Pot_ID and Zone (df = 2, 12). An auxiliary additive paired-zone test used distance ~ Pot_ID + Zone (df = 1, 14). PERMDISP used distance to spatial medians without small-sample bias correction and the same scope-specific permutation matrices. BH correction covered six marker-by-scope PERMANOVA tests and, separately, four PERMDISP tests. Alpha diversity was calculated from target-filtered counts: Shannon used natural logarithms; observed richness counted nonzero zOTUs; and classical Chao1 used singleton and doubleton counts (Section S2). NR alpha tests used Treatment + Block, and paired-zone tests used the mixed model above. Richness remains depth-sensitive

without rarefaction. Exploratory zOTU screening used a centered log-ratio transformation with a 0.5 pseudocount [15,16].

Descriptive Levins breadth was calculated for the 400 most prevalent zOTUs in each marker set [65]. For taxon i, a_{ij} was its relative abundance within profile j and $p_{ij} = a_{ij}/\Sigma_j a_{ij}$. Breadth was $B_i = 1/\Sigma_j p_{ij}^2$ across the 35 sampled profiles. Breadth describes distribution across sampled profiles; it is not a measure of resource-use breadth or a test of niche specialization.

An exploratory cross-domain screen retained the 40 most abundant bacterial and fungal features present in at least 20% of samples. CLR values were residualized for treatment–zone group and Block before calculating 1600 Spearman correlations across 35 profiles. An edge required $|\varrho| \geq 0.60$, BH $q < 0.05$, leave-one-block-out $|\varrho| \geq 0.45$ with complete sign agreement, and a permutation family-wise $p < 0.05$. The last criterion used 999 within-block permutations of the maximum absolute correlation. These permutations did not explicitly preserve paired soil profiles within each pot; the screen was therefore a diagnostic rather than a confirmatory interaction test. The absence of retained edges does not establish the absence of ecological interactions. Separate networks with five aggregated profiles per group are retained only as preliminary supplementary visualizations (Section S7; Table S11) [17–23].

Environmental associations were examined using distance-based redundancy analysis (db-RDA) [66] of the 15 amended NR profiles. The bacterial model used Catalase + SO_4^{2-} + Urease + Condition(Block); the fungal model used pH + SO_4^{2-} + Condition(Block). TOC was excluded because it reflects biochar dose, and qCO_2 was excluded because respiration incubation conditions were unavailable. The remaining terms came from an earlier exploratory candidate set and were not prespecified. Models used a Lingoes additive correction and all 7775 within-block permutations. BH correction covered the two global tests and the marginal predictors separately within each marker. Variance inflation factors, global and marginal tests, scores and axis percentages are provided in Tables S7 and S14. Descriptive Procrustes summaries and their scope limitations are provided in Table S8; no P or q values are interpreted.

Plant associations used only the 15 amended pots with matched plant, soil and microbial measurements. Standardized shoot dry weight, root dry weight or grain yield was fitted as y ~ predictor + Treatment + Block (residual df = 7). Eleven predictors were fitted separately for each response, with BH correction across all 33 tests. Soil measurements were averaged across NR and R within each pot; pot-level Shannon diversity used summed zone counts. Resource excluded CEC, and Function excluded qCO_2; the full definitions and predictor list are in Sections S1 and S8. The estimates, unadjusted 95% confidence intervals and partial R^2 are provided in Tables S12 and S14. These analyses test associations beyond treatment and block and do not establish microbial mediation. Unsuccessful structural equation models are described only as diagnostics in Section S6 and Table S10.

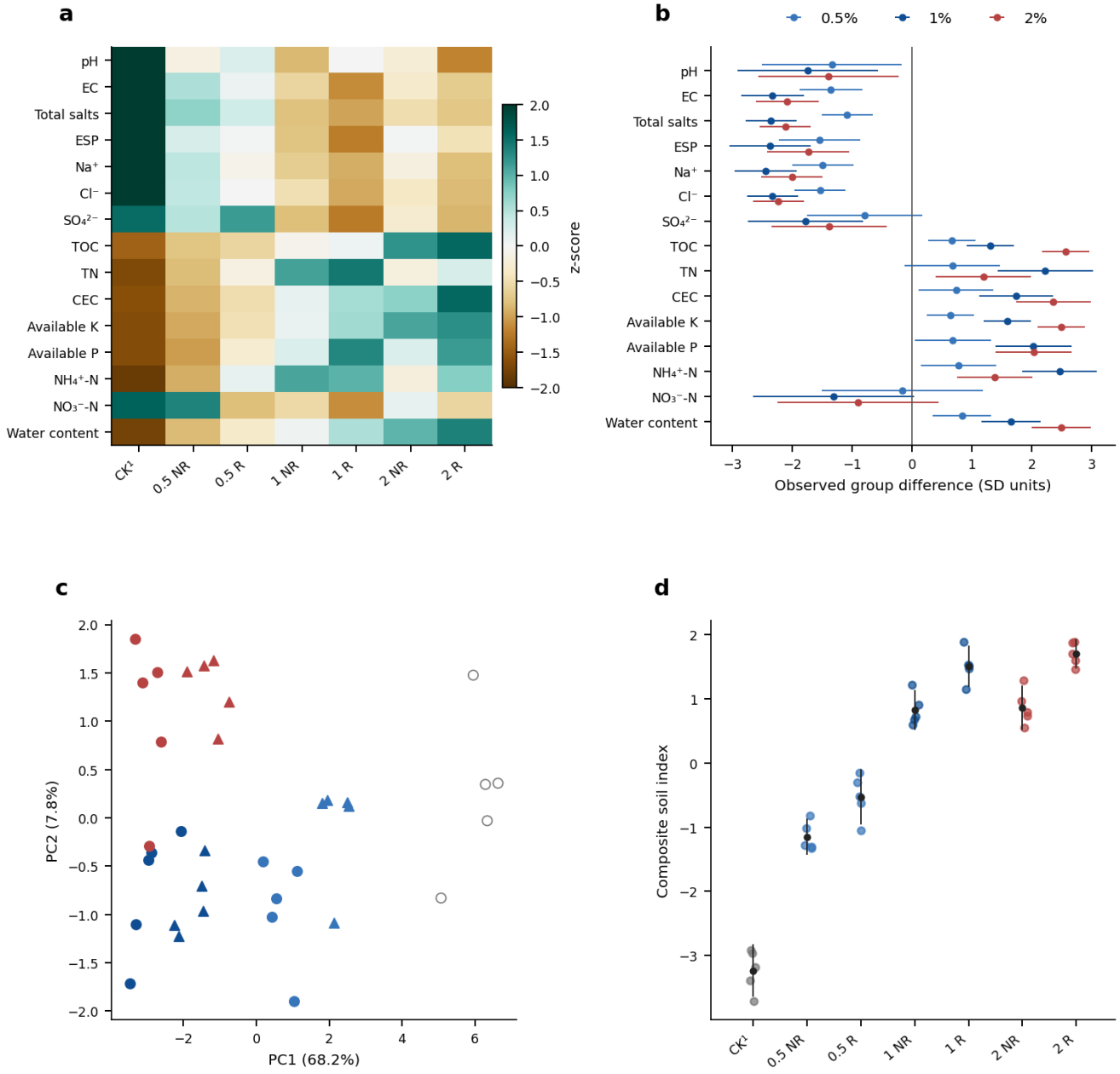
Analyses used R 4.6.0 (R Foundation for Statistical Computing, Vienna, Austria), vegan 2.7-5 and permute 0.9-10 [63,67,68]. Scripts, fixed seeds, permutation matrices, input hashes and session information accompany the Supplementary Materials. The main figures were generated from these statistical outputs using Matplotlib 3.10.9 in Python.

3. Results

3.1. Soil Properties and Maize Performance

The mean grain yield was 55.6 g plant^{-1} at 1%, 48.3 g plant^{-1} at 2% and 46.5 g plant^{-1} at 0.5%; the 1–2% difference was 7.32 g plant^{-1} (95% CI −3.52 to 18.16; q = 0.114). NR EC was 1.67, 1.08 and 1.23 dS m^{-1} at 0.5%, 1% and 2%; the value at 1% was lower than that of 0.5% (−0.58 dS m^{-1}; 95% CI −0.90 to −0.26; q = 0.0017), but that of the 1–2% difference was

uncertain (−0.15 dS m^{-1}; 95% CI −0.46 to 0.17; q = 0.205). NR pH was 8.40, 8.19 and 8.37; no pairwise difference survived correction. Plant K^+/Na^+ was 0.64, 2.26 and 2.10; the values at 1% and 2% were higher than that of 0.5% (both q < 0.001), but that of the 1–2% difference was uncertain (0.16; 95% CI −0.19 to 0.51; q = 0.205). NR TOC was 7.67, 10.78 and 16.79 g kg^{-1} at 0.5%, 1% and 2%; CK was 4.48 g kg^{-1}, but this difference included added biochar carbon and did not isolate a biological soil response. The available K for NR was 181, 270 and 354 mg kg^{-1} and for CEC was 16.0, 19.9 and 22.3 cmol kg^{-1}; CEC was reported as a measured soil–biochar mixture property and was not interpreted as biochar-derived CEC (Figure 1; Figure S1; Table S1). NO_3^--N means for NR were 372, 293 and 321 mg kg^{-1} at 0.5%, 1% and 2%, with no pairwise difference after BH correction. The corresponding NH_4^+-N means were 28.4, 45.9 and 34.7 mg kg^{-1}; that of the 1–2% contrast was 11.2 mg kg^{-1} (95% CI 1.52–20.97; q = 0.012).



¹ CK: no plant growth; bulk soil, 0–20 cm. Amended NR: 15–20 cm. NR = ▲; R = ●. Biochar rates are % (w/w).

Figure 1. Soil chemical measurements across application rates and soil zones. (**a**) Group-mean z-scores, standardized across seven groups using the population SD. Green and brown indicate

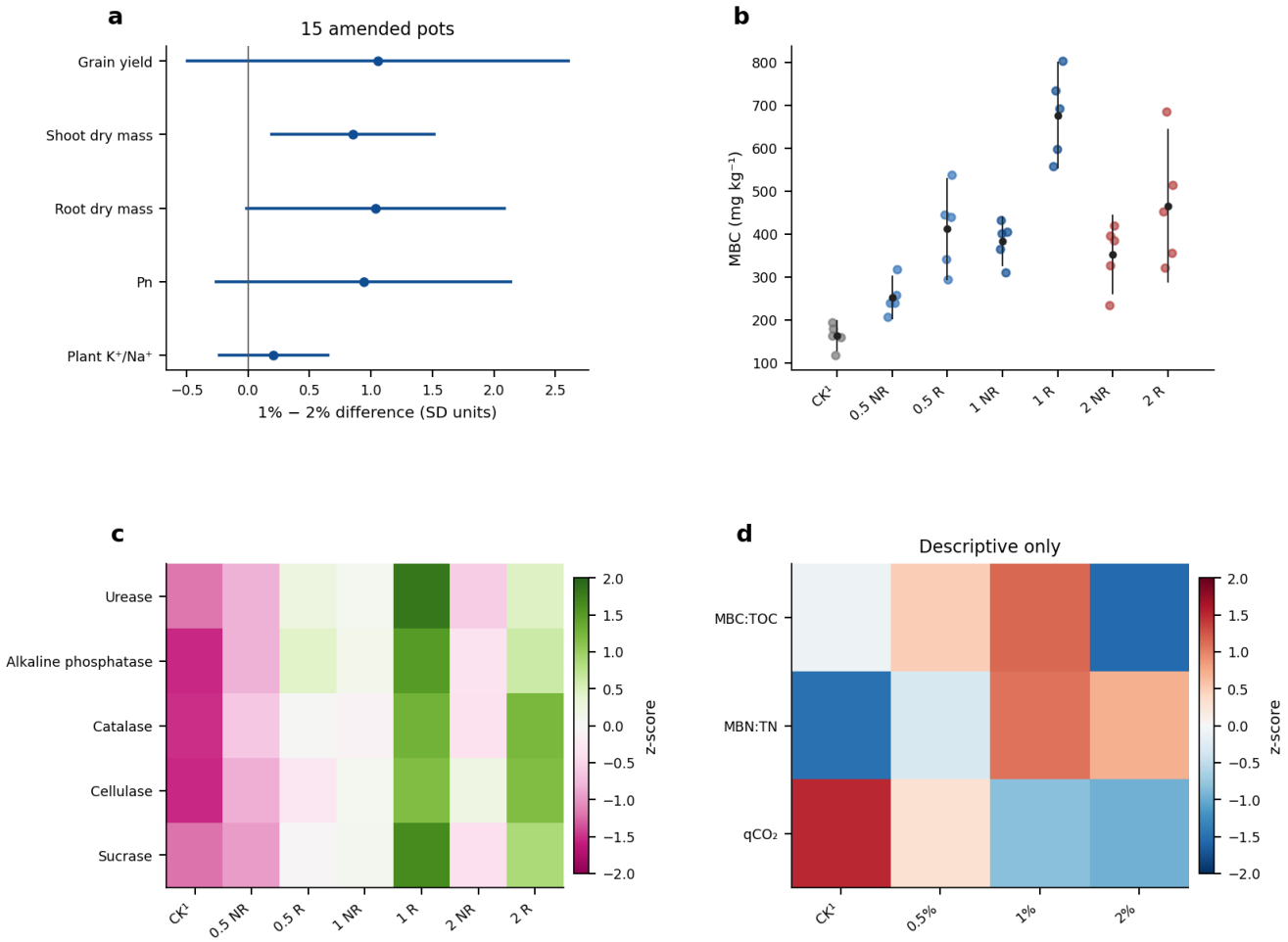
positive and negative z-scores, respectively. (**b**) Observed NR group differences from CK, with unadjusted 95% intervals, divided by the sample SD of all 20 NR profiles. CK pots contained no plants and were sampled over 0–20 cm; amended NR was sampled at 15–20 cm. (**c**) PCA of 14 variables standardized across 35 profiles: pH, EC, total salt, ESP, Na^+, Cl^-, SO_4^{2-}, TOC, TN, available K, available P, NH_4^+-N, NO_3^--N and water content. PC1 and PC2 explain 68.2% and 7.8% of total variance. In (b–d), light blue, dark blue and red denote 0.5%, 1% and 2% biochar, respectively. Filled triangles and circles in (c) denote NR and R; open gray circles in (c) and gray points in (d) denote CK. (**d**) The five-component soil-chemical index minus the seven-component salinity index, with colored observations and black points and bars denoting means and unadjusted t-based 95% intervals. LOI-derived organic matter and CEC are excluded from the index, and CEC is excluded from PCA. CK has five NR profiles; amended groups have five profiles per zone, paired within pots. This descriptive index includes added biochar carbon and is not an independently validated measure of soil health. EC, electrical conductivity; ESP, exchangeable sodium percentage; TOC, total organic carbon; TN, total nitrogen; CEC, cation exchange capacity; CK, unamended control; NR, non-rhizosphere soil; R, rhizosphere soil; LOI, loss on ignition; PCA, principal component analysis; SD, standard deviation.

The direct 1–2% comparison gave a grain-yield difference of 7.32 g $plant^{-1}$ (95% CI −3.52 to 18.16; q = 0.114). The photosynthetic rate was higher at 1% by 3.16 μmol m^{-2} s^{-1} (95% CI −0.92 to 7.24; q = 0.0475). At 2%, NR TOC was 6.01 g kg^{-1} higher than at 1% (95% CI 3.01–9.02; q = 0.0005), and available K was 84.2 mg kg^{-1} higher (95% CI 28.8–140; q = 0.0018). CEC did not differ between 1% and 2% after correction (−2.39 cmol kg^{-1}; 95% CI −5.95 to 1.17; q = 0.077). Pot-level growth, photosynthesis and ion observations are provided in Figure S2 and Table S2; current soil contrasts are in Table S14.

In the amended-only model (n = 15), the 1–2% grain-yield difference was 7.32 g $plant^{-1}$ (95% CI −3.52 to 18.16; q = 0.114). Shoot and root dry weights were higher at 1% by 25.8 g (95% CI 5.45–46.2; q = 0.0051) and 4.80 g (95% CI −0.11 to 9.71; q = 0.0229), respectively. Thus, 1% gave the highest mean yield, but its advantage over 2% was not robust.

3.2. Microbial Biomass and Enzyme Activities

The mean microbial biomass carbon (MBC) for NR was 382.9 mg kg^{-1} (95% CI 334.1–431.6) at 1% BC and 352.1 mg kg^{-1} (303.3–400.8) at 2% BC. Their difference was uncertain (30.8 mg kg^{-1}; Bonferroni 95% CI −59.4 to 121.0; q = 0.333). The urease means for NR were 700.2 and 552.1 U g^{-1}, respectively, but the 1–2% difference was not significant after BH correction (148.1 U g^{-1}; Bonferroni 95% CI −32.3 to 328.4; q = 0.0575). These use the enzyme-specific units in Section S10 and Table S3. The MBC for Rhizosphere exceeded the MBC for NR by 159.3, 293.9 and 113.6 mg kg^{-1} at 0.5%, 1% and 2%, respectively (q = 0.0066, <0.001 and 0.0283). The corresponding urease differences were 250.0, 414.9 and 240.7 U g^{-1} (all q ≤ 0.0043; Figure 2; Tables S3 and S14).



[1] CK soil is a descriptive reference; no plant growth. No CK plant observations. Rates are % (w/w).

Figure 2. Plant and microbial measurements: (**a**) 1–2% plant contrasts based on one observation per pot for 15 amended pots, with simultaneous Bonferroni 95% intervals, standardized by the sample SD across those 15 pots for each trait. (**b**) MBC observations across seven treatment–zone groups; black points and bars show means and unadjusted t-based 95% intervals. CK is a soil reference from pots without plants; there are no CK plant observations. (**c**) Enzyme group-mean z-scores standardized across seven groups using the sample SD. (**d**) Descriptive MBC:TOC, MBN:TN and qCO_2 z-scores. Ratios were calculated per profile after converting TOC and TN to mg kg^{-1}, then averaged within treatment and standardized across four means using the population SD. Each amended mean summarizes ten paired profiles; CK summarizes five NR profiles. MBC:TOC does not measure microbial carbon-use efficiency. qCO_2 is descriptive only. Amended NR and paired-zone tests are reported separately in Tables S3 and S14. TOC, total organic carbon; MBC, microbial biomass carbon; MBN, microbial biomass nitrogen; TN, total nitrogen; qCO_2, metabolic quotient (basal respiration per unit MBC); CK, unamended control; NR, non-rhizosphere soil; R, rhizosphere soil; Pn, net photosynthetic rate; SD, standard deviation.

MBC:TOC, MBN:TN and qCO_2 are shown as standardized values because their raw units differ. The TOC denominator includes added biochar carbon, so a lower MBC:TOC ratio at 2% does not by itself indicate lower microbial carbon-use efficiency. None of the 33 soil or microbial associations with plant traits survived correction after Treatment and Block were included in the 15 matched amended pots (all $q \geq 0.3097$; Table S14). Their wide confidence intervals leave uncertainty about association strength. Underlying microbial measurements are provided in Figure S3 and Table S3.

3.3. Community Composition and Diversity

Bacterial and fungal Bray–Curtis composition differed among amended rates in NR soil (Figure 3). After adjustment for Block, PERMANOVA gave $R^2 = 0.299$ and $F_{2,8} = 2.42$ for bacteria, and $R^2 = 0.653$ and $F_{2,8} = 12.53$ for fungi (both $p = 0.00077$; q = 0.00116; Table S14). The within-pot interaction tests detected rate-dependent zone differences for bacteria ($R^2 = 0.101$, $F_{2,12} = 2.69$, $p = 0.0261$, q = 0.0261) and fungi ($R^2 = 0.172$, $F_{2,12} = 9.16$, $p = 0.0018$, q = 0.00216). Mean bacterial Shannon diversity was 8.94, 8.71 and 8.95 at 0.5%, 1% and 2%; the value at 1% was lower than both other rates (both q = 0.0041). Fungal Shannon means were 3.84, 3.85 and 3.99, with no pairwise difference after correction. At 1%, fungal means were 3.85 in NR and 3.34 in R and bacterial means were 8.71 and 8.83. These tests are reported in Tables S4 and S14 and Figure S4. Shannon is a diversity index, not a richness measure.

NR treatment PERMDISP did not detect differences in spread (bacteria: $F_{2,12} = 0.83$, $p = 0.1328$, q = 0.1771; fungi: $F_{2,12} = 1.20$, $p = 0.3813$, q = 0.3813). Dispersion differed between paired zones for bacteria ($F_{1,28} = 6.07$; $p = 0.0166$; q = 0.0332) and fungi ($F_{1,28} = 65.34$; $p = 0.0001$; q = 0.0004; Table S14). The auxiliary additive paired-zone PERMANOVA gave $R^2 = 0.252$ for bacteria ($F_{1,14} = 10.80$; $p = 0.0001$) and $R^2 = 0.307$ for fungi ($F_{1,14} = 15.09$; $p = 0.0003$). These zone differences may reflect community spread as well as average composition. A larger fungal R^2 does not by itself establish a stronger biological response.

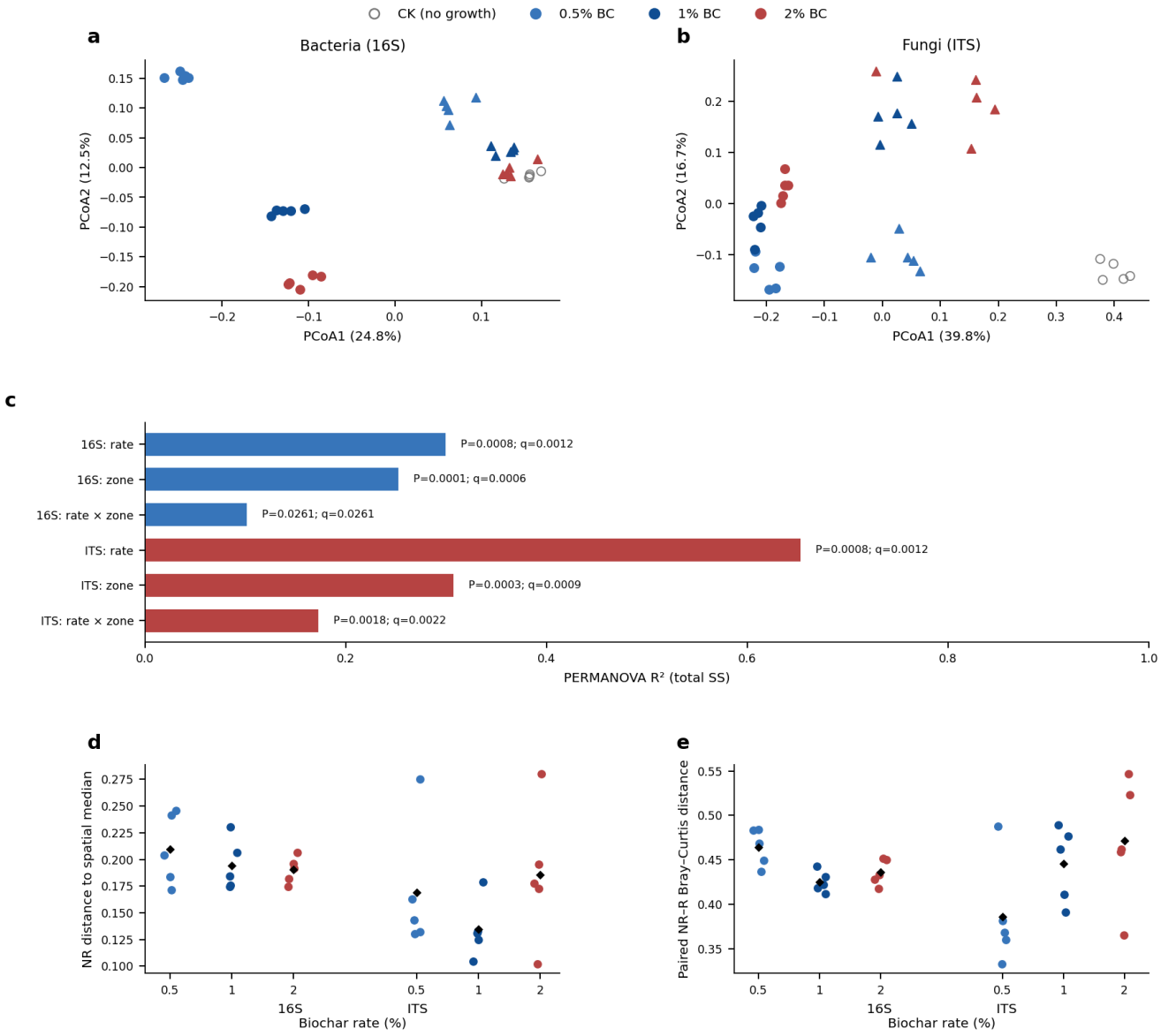
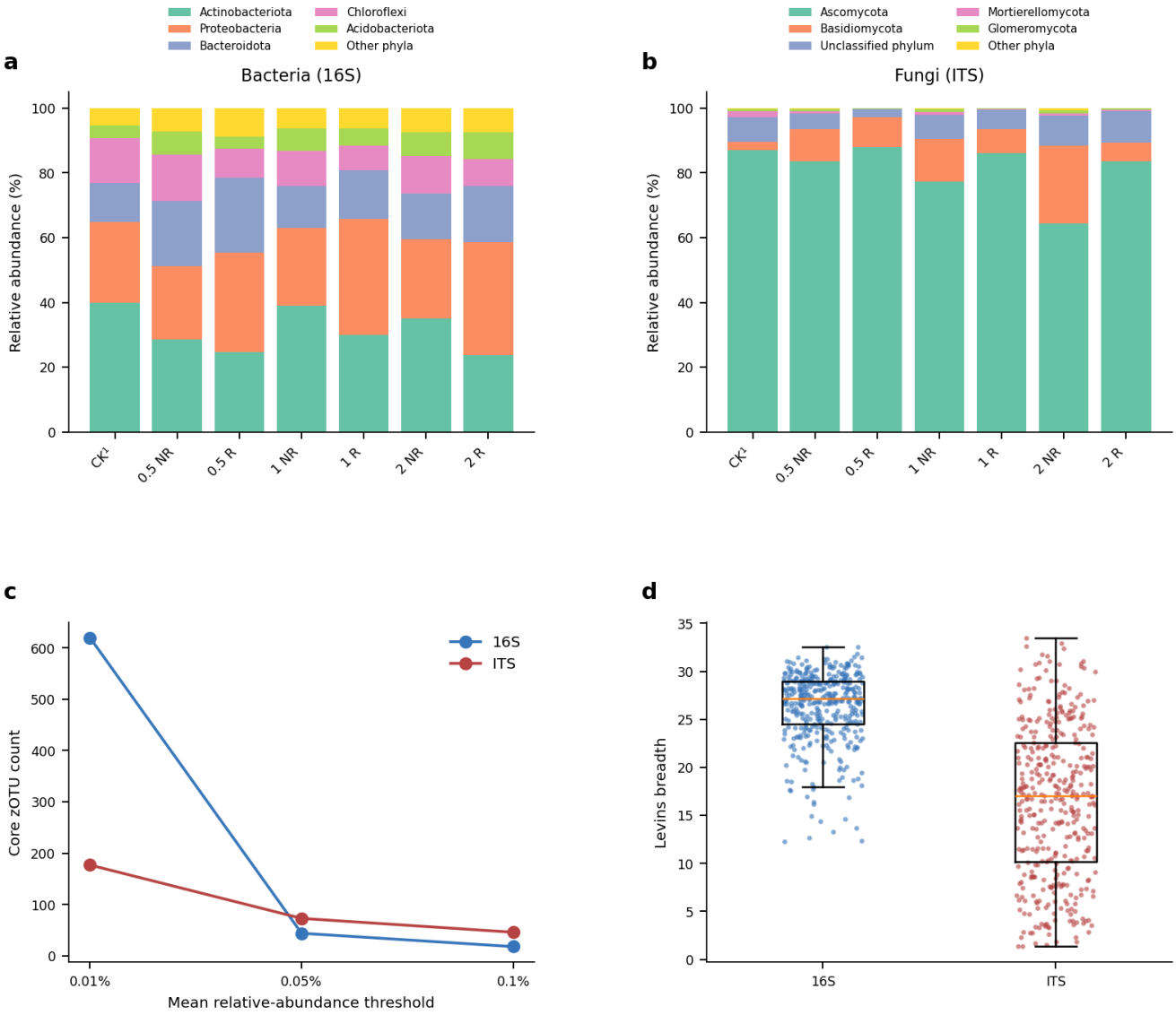


Figure 3. Bacterial and fungal composition and dispersion. (**a**,**b**) Bray–Curtis PCoA of 35 target-filtered profiles per marker; percentages are based on positive eigenvalues. Gray open circles denote CK pots without plants; light blue, dark blue and red denote 0.5%, 1% and 2% BC. Triangles denote amended NR and circles R. (**c**) PERMANOVA R^2 as a proportion of total sums of squares, with restricted-permutation P and BH q. Rate tests use 15 amended NR profiles with Block; paired tests use 30 amended profiles with Pot_ID, and the interaction is tested after Pot_ID and Zone. (**d**) Distances to spatial medians using only the 15 amended NR profiles per marker. (**e**) Direct within-pot NR–R Bray–Curtis distances for the 15 amended pots. Points represent observations; black diamonds in d/e mark descriptive means. Composition tests must be interpreted with the dispersion diagnostics.

3.4. Taxonomic Composition

At 1% BC, Proteobacteria accounted for 24.15% of bacterial reads in NR and 35.77% in R, whereas Actinobacteriota accounted for 38.94% and 29.98%, respectively. At 2%, the corresponding proportions were 24.52% and 34.97% for Proteobacteria, and 34.95% and 23.68% for Actinobacteriota. Fungal Ascomycota and Basidiomycota represented 86.97% and 2.66% in CK. In amended NR, their proportions changed from 77.44% and 13.06% at 1% to 64.30% and 24.07% at 2%; the 2% R values were 83.52% and 5.84%. The fungal rate-

by-zone interaction ($R^2 = 0.172$, $p = 0.0018$) is consistent with zone-dependent composition. These are mean relative abundances from confidence-filtered phylum assignments, not absolute cell counts or evidence of functional guilds (Figure 4).



¹ CK: no plant growth. Panels c/d describe taxa across 35 profiles; taxa are not independent pot replicates.

Figure 4. Taxonomic composition and distribution across sampled soil profiles. (**a**,**b**) Mean bacterial and fungal composition across seven treatment–zone groups, with five profiles per group; unsupported phylum assignments are grouped as unclassified. (**c**) Core-zOTU counts: mean relative abundance must reach the indicated threshold, and abundance must reach that threshold in at least 80% of the 35 profiles. Thresholds of 0.0001, 0.0005 and 0.001 correspond to 0.01%, 0.05% and 0.1%. In (c,d), blue and red denote bacteria (16S) and fungi (ITS), respectively. (**d**) Levins breadth [65] for the 400 most prevalent zOTUs per marker across all 35 profiles. Orange lines indicate medians and boxes show interquartile ranges; whiskers extend to the most extreme values within 1.5 interquartile ranges. Points are taxa, not independent soil samples. Breadth describes distribution across observed profiles, not measured resource use.

The core-taxon counts and Levins breadth provide descriptive comparisons across the sampled profiles. Exploratory zOTU screening and dominant-taxon summaries are provided in Table S5 and Figure S5; they are not presented as validated biomarkers. Restricted community-test results are summarized in Figure S6. The bacterial phylogenetic

sensitivity diagnostic is shown in Figure S7 and Tables S6 and S13; threshold exceedance describes numerical sensitivity, not ecological-process proportions. Abundance-class summaries are provided in Figure S8 and Table S5. The exploratory cross-domain correlation-screen diagnostic is shown in Figure S9 and Table S9; no edge met all screening criteria, and the permutation scheme did not explicitly preserve paired profiles.

3.5. Soil–Community Associations

Amended-only db-RDA without TOC or qCO_2 explained limited variation. The bacterial model had adjusted $R^2 = 0.075$ (global $F_{3,7} = 1.24$, $p = 0.0481$, q = 0.0962); the fungal model had adjusted $R^2 = 0.137$ (global $F_{2,8} = 1.65$, $p = 0.1134$, q = 0.1134). Neither global model passed BH correction across the two markers. No bacterial predictor passed within-model correction. Fungal SO_4^{2-} had a marginal $p = 0.0153$ and q = 0.0306, but the nonsignificant global model and prior variable selection limit this to an exploratory association (Figure 5; Tables S7 and S14). Marginal model tests are shown in Figure S10. Preliminary bacteria–fungi, bacterial and fungal correlation plots are presented in Figures S11–S13, respectively, with grouping definitions and interpretation limits in Table S11. Their displayed topology is sensitive to aggregation and sample size and is not evidence of ecological interaction or stability.

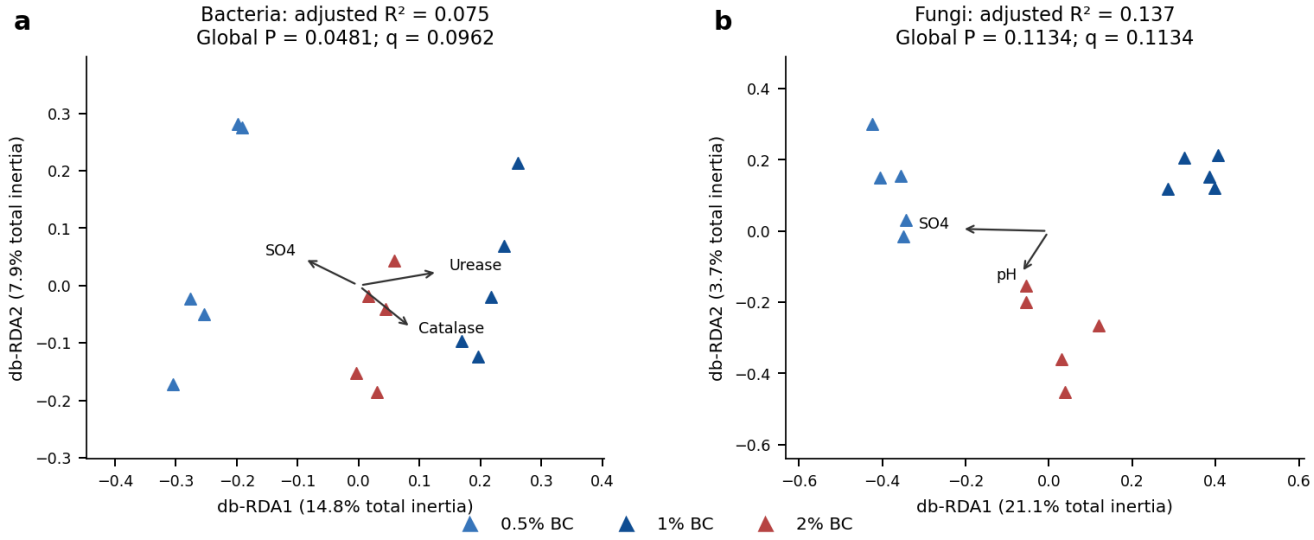


Figure 5. Amended-only NR soil–community associations. (**a**,**b**) Bacterial and fungal Bray–Curtis db-RDA for 15 amended NR profiles, conditioned on Block and using a Lingoes additive correction. The bacterial model uses catalase, SO_4^{2-} and urease; the fungal model uses pH and SO_4^{2-}. TOC and qCO_2 are excluded. Light blue, dark blue and red triangles represent the 0.5%, 1% and 2% biochar (BC) treatments, respectively. Arrows show environmental predictors; axis percentages refer to total inertia. Adjusted R^2, global restricted-permutation P and BH q across the two markers are shown. Tests enumerate 7775 within-block permutations. Neither global model passes BH correction. Marginal tests are shown in Figure S10 and Tables S7 and S14.

4. Discussion

4.1. Microbial Responses Across Application Rates and Soil Zones

The compositional responses differed between bacteria and fungi and between the two soil zones. Proteobacteria occupied a larger proportion of bacterial reads in R than NR at 1% and 2% BC, while Actinobacteriota showed the opposite pattern. Higher rhizosphere MBC at all three rates indicates that the zone contrast extended beyond relative-

abundance profiles. Root inputs and altered local nutrient conditions offered plausible explanations [14], but their contribution was not quantified. The fungal shift toward Basidiomycota was most pronounced in 2% NR. The Treatment × Zone interaction supports zone-dependent community responses, but dispersion differences mean that changes in average composition and variability cannot be fully separated.

Two design features limit interpretation: CK had no plants, and CK and amended NR soil were sampled at different depths. CK pots contained no plants and were sampled as a 0–20 cm composite, whereas amended NR soil was sampled at 15–20 cm; CK–amended differences therefore combined plant presence and sampling depth and were reported as observed group differences. No CK rhizosphere sample was available, so an unamended rhizosphere effect could not be estimated. Dispersion differed between the paired zones for both markers, meaning that changes in average composition and community variability could not be fully separated in those tests [62,64]. Community shifts also do not establish changes in metabolic activity.

4.2. Carbon Input and Soil Chemical Changes

The measured TOC increase should not be interpreted as newly formed native soil organic carbon. NR TOC was 7.67, 10.78 and 16.79 g kg^{-1} at 0.5%, 1% and 2%, compared with 4.48 g kg^{-1} in CK. The shared material record reports a biochar TOC of 63.14% [24]; multiplying this fraction by the three rates gives nominal inputs of 3.16, 6.31 and 12.63 g organic C per kg original soil. The observed increments (3.19, 6.30 and 12.31 g kg^{-1}) correspond to 101%, 99.8% and 97.5% of these inputs. This comparison is consistent with a substantial direct contribution from the amendment. It is not a strict carbon balance, because source-specific recovery, final mixture mass and carbon losses were not quantified.

Biochar surfaces and mineral ash may contribute to CEC and extractable K, but those contributions were not separated experimentally. The observed CEC increments (2.833, 6.718 and 9.110 cmol kg^{-1}) were 16–24 times the nominal additive estimates obtained from the reported biochar CEC (0.143, 0.285 and 0.570 cmol kg^{-1}). Soil CEC was measured by hexamminecobalt extraction, whereas biochar CEC was measured by NH_4OAc at pH 7. These different methods prevent treating the additive estimates as a strict upper bound or a direct analytical validation. Original photometric absorbances, initial and final solution concentrations, calibration and blank records were unavailable for independent verification of the soil CEC values. CEC was therefore excluded from the composite index and not interpreted as biochar-derived exchange capacity.

TOC, CEC and available K were higher at 2%, but these were mixture properties, not evidence of biologically generated soil resources. MBC:TOC has the same limitation: adding biochar carbon increases its denominator even if microbial biomass is unchanged. A lower ratio therefore cannot establish lower microbial carbon-use efficiency. Comparisons among application rates should retain the separate chemical, microbial and plant measurements instead of assigning a single biological meaning to a composite soil index.

4.3. Soil–Community Associations and Uncertainty

The amended-only environmental models explained limited variation, and neither global test passed correction across the two markers. The marginal fungal SO_4^{2-} association should therefore be treated cautiously. Correlated soil properties, prior variable selection and five pots per rate limit attribution to particular variables. These exploratory associations do not distinguish direct effects of biochar from changes mediated by roots, salinity, water or nutrient supply.

MBC and MBN quantify extractable microbial biomass pools, enzyme assays measure potential activity, and qCO_2 expresses basal respiration per unit microbial biomass [45–47]. None are a direct measure of microbial carbon-use efficiency. These

measurements describe the biological soil response; their association with community composition does not establish a link to maize yield. Candidate zOTUs likewise require independent validation because the abundance data are compositional and marker-specific [16].

4.4. Maize Responses and Possible Nitrogen Constraints

The 1% treatment produced the highest mean grain yield and photosynthetic rate, whereas several soil chemical means were highest at 2%. The yield difference was uncertain ($q = 0.114$), so the data did not establish 1% as an optimal rate. Mean MBC and urease were higher at 1% than at 2%, but neither contrast passed endpoint-specific BH correction. Treatment-adjusted associations did not identify an additional microbial contribution to plant performance; their confidence intervals were wide, so a contribution could not be excluded.

Reported extractable mineral-N concentrations were high at all rates. NO_3^--N was 293 mg kg^{-1} at 1% and 321 mg kg^{-1} at 2%, while NH_4^+-N was higher at 1% than at 2% (45.9 versus 34.7 mg kg^{-1}; $q = 0.012$). Nitrate was not lower at 2%, but the measurements did not quantify N transformation rates or a plant N balance. Original analytical records are needed to resolve the high nitrate fraction of TN. Differences in water availability, nutrient balance or rooting conditions remain possible explanations for plant responses, without establishing a mechanism.

Han et al. [69] tested maize-straw biochar, desulfurized gypsum (a non-carbon amendment) and their combination in salinized soil. Wang et al. [70] followed a single biochar application in a three-year cotton pot experiment and found responses that varied with rate and year. These studies differ in crop, amendment and nutrient management and do not establish a generally optimal rate for maize. Field evaluation should measure crop performance alongside salinity, nutrient availability and the carbon directly added with the amendment.

Soil pH and EC were not lower at 2% than at 1% after correction (pH $q = 0.85$; EC $q = 0.205$), and the CK–amended differences were confounded by plant presence and sampling depth. The alkaline biochar (pH 9.52) therefore does not provide evidence of a biochar-driven pH decline in these pots. pHpzc (8.2) describes zero net surface charge under the assay conditions, not a target pH for the soil mixture.

4.5. Limitations and Field Validation

This experiment used one soil, one maize cultivar, five blocks and a single harvest. The 20-pot design comprised 15 amended pots and five CK soil pots without plants; CK was sampled over 0–20 cm, whereas amended NR soil was taken at 15–20 cm, so CK–amended differences combine plant presence and depth. No CK rhizosphere sample was available. The 8 kg soil mass and 20 cm pots restricted rooting space and may have altered water movement and salt redistribution compared with field soil. Plant number differed among treatments. The analysis uses within-pot plant means, but pot-specific plant counts were not available in the analysis dataset, so effects associated with plant density could not be separated from the observed rate differences. A single harvest cannot show whether the responses persisted or how they developed over time. Shared samples with the companion study [24] also limit the independence of the evidence. The environmental models remain exploratory. Initial nutrient concentrations, ESP and texture were not measured, and the initial EC extraction ratio was not recorded. Harvest was based on visual assessment rather than a physiological-maturity test, and air-dried grain was not standardized for moisture. Missing respiration incubation conditions limited the interpretation of qCO_2, and qCO_2 was not used as a predictor. The high extractable-nitrate fraction also constrains inference about soil N transformations.

Future experiments need planted controls sampled at matching depths, documented plant numbers and harvest criteria, repeated sampling, complete analytical calibration records and larger rooting volumes. Such designs could separate amendment, rhizosphere and sampling-depth effects while testing whether measured microbial changes contribute to crop performance.

5. Conclusions

Across the tested rates, 1% BC gave the highest mean maize yield (55.6 g plant^{-1}), but the 1–2% difference was uncertain (7.32 g plant^{-1}; Bonferroni 95% CI −3.52 to 18.16; BH q = 0.114). NR EC was lower at 1% than at 0.5% (q = 0.0017) but did not differ between 1% and 2% (q = 0.205). Bacterial and fungal composition differed among amended rates, with within-pot rate-by-zone interactions; dispersion differences limited the interpretation of zone effects. Neither environmental db-RDA model passed global BH correction, and no treatment-adjusted soil–plant association survived correction. At 2%, the observed NR TOC increment above CK was close to nominal biochar carbon input and did not demonstrate an increase in native soil carbon. Higher chemical measurements at 2% did not coincide with the highest mean yield. Field trials with matched planted controls are needed to establish agronomically suitable application rates.

Supplementary Materials: The following supporting information can be downloaded at https://www.mdpi.com/article/10.3390/life16111781/s1. Sections S1–S10 provide additional methods and reproducibility information. Figure S1: Soil salinity, ions and chemical measurements across seven groups; Figure S2: Pot-level plant observations from 15 amended pots, with five pots at each rate; Figure S3: Enzyme activities, microbial biomass and qCO_2 across seven soil groups; Figure S4: Alpha diversity of amended bacterial and fungal profiles only; Figure S5: Dominant target-filtered bacterial and fungal zOTUs by mean relative abundance across 35 profiles; Figure S6: Restricted community tests; Figure S7: Bacterial phylogenetic numerical sensitivity; Figure S8: Target-filtered rare, intermediate and abundant zOTU counts; Figure S9: Exploratory bacteria–fungi correlation-screen diagnostic; Figure S10: Amended-only NR environmental models; Figure S11: Preliminary bacteria–fungi correlation plots for CK non-rhizosphere soil, biochar non-rhizosphere soil and biochar rhizosphere soil; Figure S12: Preliminary bacterial correlation plots for CK non-rhizosphere soil and the two amended-soil zones; Figure S13: Preliminary fungal correlation plots for CK non-rhizosphere soil and the two amended-soil zones, using five profiles per group. Table S1: Soil observations, amended NR means and contrasts, paired-zone contrasts, descriptive CK differences and method limitations; Table S2: Plant observations from 15 amended pots and Treatment+Block estimated means/contrasts; Table S3: Enzyme and microbial-biomass observations, amended NR/paired-zone models, descriptive CK differences, and assay-specific definitions; Table S4: Target-filtered alpha-diversity observations, amended NR rate tests, paired-zone models, PERMANOVA and PERMDISP; Table S5: Recomputed dominant taxa, core counts, Levins breadth and abundance classes, plus explicitly exploratory earlier CLR-screen diagnostics; Table S6: Bacterial numerical phylogenetic sensitivity: retained coverage and dependent pairwise values only; no ecological-process inference; Table S7: Current amended-only NR db-RDA global/marginal tests, VIF, site/arrow scores and axes; Table S8: Descriptive Procrustes concordance with scope limitations; no P or q values and no inference of microbial interaction; Table S9: Cross-domain residual-correlation diagnostics, null distributions and interpretation limits; Table S10: Current analysis/software/figure status and reasons that unsuccessful SEM results do not support causal interpretation; invalid model coefficients are excluded; Table S11: Preliminary network metrics, grouping definitions and interpretation limits for Figures S11–S13; Table S12: Treatment+Block-adjusted associations using 15 matched amended pots, analysis inputs and the cross-endpoint multiplicity sensitivity; Table S13: Matched bacterial sensitivity series at 55.01%, 80.00% and 100% read coverage; 595 dependent pairs per level, 999 shuffles; Table S14: Consolidated R5 statistics: amended-rate and paired-zone

effects, descriptive CK contrasts, alpha diversity, restricted community tests, db-RDA, indices, arithmetic, matched-pot associations and explicit BH families; Table S15: Pot-level design and sample audit. Tables S1–S15 are supplied as separate Excel files in the 03_Tables folder. The 01_Supplementary_Materials.docx and .pdf files contain Sections S1–S10, Figures S1–S13 and the table descriptions. The 02_Figures folder contains the 13 supplementary TIFF figures. Sample metadata are in 04_Sample_Metadata/05_Sample_Metadata.xlsx. Data_and_Code.zip, R4R2_Data_and_Code_Addendum.zip and FASTQ_manifest.csv are in 05_Data_and_Code; the second archive retains its filename for continuity and contains the current scripts and outputs. SHA256SUMS.txt lists file checksums. References [24,44–47,50–57,71–74] are cited in the Supplementary Materials.

Author Contributions: C.Z.: Investigation, Formal analysis, Data curation, Visualization, Writing—original draft. Y.M.: Investigation, Methodology, Data curation. F.L.: Investigation, Methodology, Validation. G.Z.: Investigation, Data curation. Q.S.: Investigation (soil and plant measurements), Validation. T.H.: Formal analysis (microbial analysis), Data curation. Z.P.: Software, Visualization, Data curation. X.L.: Methodology, Resources, Writing—review and editing. R.L.: Conceptualization, Supervision, Project administration, Funding acquisition, Writing—review and editing. All authors have read and agreed to the published version of the manuscript.

Funding: This work was supported by the Pilot Program of the Scientific Research Fund of BGRIMM Technology Group (Grant No. 02-2418), the National Key R&D Program of China (Grant Nos. 2022YFC2903904 and 2025YFC3715205), and the Youth Science and Technology Innovation Fund of BGRIMM Technology Group (Grant No. 04-2512).

Institutional Review Board Statement: Not applicable.

Informed Consent Statement: Not applicable.

Data Availability Statement: The sequencing project is registered in the Genome Sequence Archive under BioProject accession PRJCA066142: https://ngdc.cncb.ac.cn/bioproject/browse/PRJCA066142 (accessed on 22 October 2026). A public CRA accession and record link are pending release. Reviewer access will be provided through the journal submission system. Processed count tables, current measurement inputs and FASTQ_manifest.csv are provided in the Supplementary 05_Data_and_Code folder; raw FASTQ files are intended for GSA and are not included in the Supplementary ZIP. Data_and_Code.zip contains the analysis inputs, and R4R2_Data_and_Code_Addendum.zip contains the R5 scripts, statistical outputs, permutation matrices and software records. Metadata are in 04_Sample_Metadata/05_Sample_Metadata.xlsx, and consolidated statistics are in 03_Tables/Table_S14.xlsx.

Acknowledgments: The authors thank the staff of the greenhouse agricultural base in Xiong'an New Area for assistance with pot management and sampling and the colleagues at BGRIMM Technology Group for laboratory support.

Conflicts of Interest: Chi Zhang, Yu Miao, Fangze Li, Ge Zhang, Qiwei Sun, Tianci Hua, Zhikun Pang, Xingjie Lin and Rui Li are employees of BGRIMM Technology Group, a research-oriented company. The authors declare no other conflicts of interest.

References

1. Richards, L.A. (Ed.) *Diagnosis and Improvement of Saline and Alkali Soils*; USDA Agriculture Handbook 60; USDA: Washington, DC, USA, 1954.
2. Rengasamy, P. Soil processes affecting crop production in salt-affected soils. *Funct. Plant Biol.* **2010**, *37*, 613–620. https://doi.org/10.1071/FP09249.
3. Rath, K.M.; Fierer, N.; Murphy, D.V.; Rousk, J. Linking bacterial community composition to soil salinity along environmental gradients. *ISME J.* **2019**, *13*, 836–846. https://doi.org/10.1038/s41396-018-0313-8.
4. National Development and Reform Commission. Reply to Recommendation No. 6966 of the Fifth Session of the Twelfth National People's Congress (2017). Published Online 8 July 2021. Available online: https://www.ndrc.gov.cn/xxgk/jianyitianfuwen/qgrddbjyfwgk/202107/t20210708_1288484.html (accessed on 19 October 2026).
5. Zhang, Z.; Fan, Y.; Jiao, Z.; Guan, Q. Impact of soil salinization on the eco-environment quality of coastal wetlands: A case study of Yellow River Delta. *Remote Sens. Nat. Resour.* **2023**, *35*, 226–235. https://doi.org/10.6046/zrzyyg.2022284. Available online: https://www.gtzyyg.com/en/article/doi/10.6046/zrzyyg.2022284 (accessed on 22 October 2026).
6. Saifullah; Dahlawi, S.; Naeem, A.; Rengel, Z.; Naidu, R. Biochar application for the remediation of salt-affected soils: Challenges and opportunities. *Sci. Total Environ.* **2018**, *625*, 320–335. https://doi.org/10.1016/j.scitotenv.2017.12.257.
7. Su, Z.; Liu, X.; Wang, Z.; Wang, J. Biochar effects on salt-affected soil properties and plant productivity: A global meta-analysis. *J. Environ. Manag.* **2024**, *366*, 121653. https://doi.org/10.1016/j.jenvman.2024.121653.
8. Liu, J.; Shi, Z.; Zhang, L.; Feng, R.; Zhang, G.; Zou, H.; Wang, G.; Yang, Y. Contrasting acidic and alkaline biochar reprogram alfalfa metabolism and rhizosphere microbiomes in saline-alkali soils. *Biochar* **2026**, *8*, 82. https://doi.org/10.1007/s42773-026-00595-y.
9. Murtaza, G.; Rizwan, M.; Usman, M.; Hyder, S.; Akram, M.I.; Deeb, M.; Alkahtani, J.; AlMunqedhi, B.M.; Hendy, A.S.; Ali, M.R.; et al. Biochar enhances the growth and physiological characteristics of Medicago sativa, Amaranthus caudatus and Zea mays in saline soils. *BMC Plant Biol.* **2024**, *24*, 304. https://doi.org/10.1186/s12870-024-04957-1.
10. Deshoux, M.; Sadet-Bourgeteau, S.; Gentil, S.; Prévost-Bouré, N.C. Effects of biochar on soil microbial communities: A meta-analysis. Sci. *Total Environ.* **2023**, *902*, 166079. https://doi.org/10.1016/j.scitotenv.2023.166079.
11. Li, X.; Wang, T.; Chang, S.X.; Jiang, X.; Song, Y. Biochar increases soil microbial biomass but has variable effects on microbial diversity: A meta-analysis. *Sci. Total Environ.* **2020**, *749*, 141593. https://doi.org/10.1016/j.scitotenv.2020.141593.
12. Wang, Z.; Wang, H.; Zhao, C.; Yang, K.; Li, Z.; Yin, K. Effects of biochar on the microenvironment of saline-sodic soil and maize growth. *Agronomy* **2022**, *12*, 2859. https://doi.org/10.3390/agronomy12112859.
13. Zhu, B.; Li, J.; Li, J.; Chen, X.; Chi, G. Fungal community is more sensitive to the short-term application of biochar in saline farmland soil than bacterial community. *Appl. Soil Ecol.* **2025**, *212*, 106219. https://doi.org/10.1016/j.apsoil.2025.106219.
14. Ling, N.; Wang, T.; Kuzyakov, Y. Rhizosphere bacteriome structure and functions. *Nat. Commun.* **2022**, *13*, 836. https://doi.org/10.1038/s41467-022-28448-9.
15. Aitchison, J. The statistical analysis of compositional data. *J. R. Stat. Soc. Ser. B* **1982**, *44*, 139–177. https://doi.org/10.1111/j.2517-6161.1982.tb01195.x.
16. Gloor, G.B.; Macklaim, J.M.; Pawlowsky-Glahn, V.; Egozcue, J.J. Microbiome datasets are compositional: And this is not optional. *Front. Microbiol.* **2017**, *8*, 2224. https://doi.org/10.3389/fmicb.2017.02224.
17. Friedman, J.; Alm, E.J. Inferring correlation networks from genomic survey data. *PLoS Comput. Biol.* **2012**, *8*, e1002687. https://doi.org/10.1371/journal.pcbi.1002687.
18. Kurtz, Z.D.; Müller, C.L.; Miraldi, E.R.; Littman, D.R.; Blaser, M.J.; Bonneau, R.A. Sparse and compositionally robust inference of microbial ecological networks. *PLoS Comput. Biol.* **2015**, *11*, e1004226. https://doi.org/10.1371/journal.pcbi.1004226.
19. Weiss, S.; Van Treuren, W.; Lozupone, C.; Faust, K.; Friedman, J.; Deng, Y.; Xia, L.C.; Xu, Z.Z.; Ursell, L.; Alm, E.J.; et al. Correlation detection strategies in microbial data sets vary widely in sensitivity and precision. *ISME J.* **2016**, *10*, 1669–1681. https://doi.org/10.1038/ismej.2015.235.
20. Röttjers, L.; Faust, K. From hairballs to hypotheses—Biological insights from microbial networks. *FEMS Microbiol. Rev.* **2018**, *42*, 761–780. https://doi.org/10.1093/femsre/fuy030.
21. Carr, A.; Diener, C.; Baliga, N.S.; Gibbons, S.M. Use and abuse of correlation analyses in microbial ecology. *ISME J.* **2019**, *13*, 2647–2655. https://doi.org/10.1038/s41396-019-0459-z.
22. Faust, K. Open challenges for microbial network construction and analysis. *ISME J.* **2021**, *15*, 3111–3118. https://doi.org/10.1038/s41396-021-01027-4.

23. Liu, C.; Li, C.; Jiang, Y.; Zeng, R.J.; Yao, M.; Li, X. A guide for comparing microbial co-occurrence networks. *iMeta* **2023**, *2*, e71. https://doi.org/10.1002/imt2.71.
24. Li, R.; Zhang, C.; Miao, Y.; Li, F.; Zhang, G.; Sun, Q.; Hua, T.; Pang, Z.; Lin, X. Biochar-Associated Shifts in Nitrogen Status, Microbial Communities and Dissolved Organic Matter in Salt-Affected Maize Soil. *Microorganisms* **2026**, *14*, 1907. https://doi.org/10.3390/microorganisms14091907.
25. Lu, R.K. *Methods of Soil and Agro-Chemical Analysis*; China Agricultural Science and Technology Press: Beijing, China, 2000.
26. Bao, S.D. *Soil and Agricultural Chemistry Analysis*; China Agriculture Press: Beijing, China, 2000.
27. Rhoades, J.D. Salinity: Electrical conductivity and total dissolved solids. In *Methods of Soil Analysis, Part 3: Chemical Methods*; Sparks, D.L., Ed.; Soil Science Society of America: Madison, WI, USA, 1996; pp. 417–435.
28. *NY/T 1121.16-2006*; Soil Testing—Part 16: Method for Determination of Total Water-Soluble Salt. Ministry of Agriculture: Beijing, China; Ministry of Agriculture of the People's Republic of China: Beijing, China, 2006.
29. Olsen, S.R.; Cole, C.V.; Watanabe, F.S.; Dean, L.A. *Estimation of Available Phosphorus in Soils by Extraction with Sodium Bicarbonate; USDA Circular 939*; USDA: Washington, DC, USA, 1954.
30. *HJ 704-2014*; Soil Quality—Determination of Available Phosphorus—Sodium Hydrogen Carbonate Solution-Mo-Sb Anti Spectrophotometric Method. Ministry of Environmental Protection: Beijing, China; Ministry of Environmental Protection of the People's Republic of China: Beijing, China, 2014.
31. *NY/T 889-2004*; Determination of Exchangeable Potassium and Non-Exchangeable Potassium Content in Soil. Ministry of Agriculture: Beijing, China; Ministry of Agriculture of the People's Republic of China: Beijing, China, 2005.
32. *HJ 761-2015*; Solid Waste—Determination of Organic Matter—Ignition Loss Method. Ministry of Environmental Protection: Beijing, China; Ministry of Environmental Protection of the People's Republic of China: Beijing, China, 2015.
33. Hoogsteen, M.J.J.; Lantinga, E.A.; Bakker, E.J.; Groot, J.C.J.; Tittonell, P.A. Estimating soil organic carbon through loss on ignition: Effects of ignition conditions and structural water loss. *Eur. J. Soil Sci.* **2015**, *66*, 320–328. https://doi.org/10.1111/ejss.12224.
34. *HJ 634-2012*; Soil—Determination of Ammonium, Nitrite and Nitrate by Extraction with Potassium Chloride Solution—Spectrophotometric Methods. Ministry of Environmental Protection: Beijing, China; Ministry of Environmental Protection of the People's Republic of China: Beijing, China, 2012.
35. *GB/T 32737-2016*; Soil Quality—Determination of Nitrate—Ultraviolet Spectrophotometric Method; Standards Press of China: Beijing, China; General Administration of Quality Supervision, Inspection and Quarantine: Beijing, China; Standardization Administration of China: Beijing, China, 2016.
36. *HJ 636-2012*; Water Quality—Determination of Total Nitrogen—Alkaline Potassium Persulfate Digestion UV Spectrophotometric Method. Ministry of Environmental Protection: Beijing, China; Ministry of Environmental Protection of the People's Republic of China: Beijing, China, 2012.
37. *HJ 889-2017*; Soil Quality—Determination of Cation Exchange Capacity (CEC)—Hexamminecobalt Trichloride Solution-Spectrophotometric Method. Ministry of Environmental Protection: Beijing, China; Ministry of Environmental Protection of the People's Republic of China: Beijing, China, 2017.
38. *HJ 832-2017*; Soil and Sediment—Digestion of Total Metal Elements—Microwave Assisted Acid Digestion Method. Ministry of Environmental Protection: Beijing, China; Ministry of Environmental Protection of the People's Republic of China: Beijing, China, 2017.
39. Lichtenthaler, H.K.; Wellburn, A.R. Determinations of total carotenoids and chlorophylls a and b of leaf extracts in different solvents. *Biochem. Soc. Trans.* **1983**, *11*, 591–592. https://doi.org/10.1042/bst0110591.
40. Kandeler, E.; Gerber, H. Short-term assay of soil urease activity using colorimetric determination of ammonium. *Biol. Fertil. Soils* **1988**, *6*, 68–72. https://doi.org/10.1007/BF00257924.
41. Beijing Solarbio Science & Technology Co., Ltd. Soil Alkaline Phosphatase Activity Assay Kit: Phenylphosphate/Phenol-Release Method. Available online: https://www.solarbio.com/goodsInfo?id=9135 (accessed on 19 October 2026).
42. Tabatabai, M.A. Soil enzymes. In *Methods of Soil Analysis, Part 2: Microbiological and Biochemical Properties*; Weaver, R.W.; Angle, J.S.; Bottomley, P.S., Eds.; Soil Science Society of America: Madison, WI, USA, 1994; pp. 775–833.
43. Alef, K.; Nannipieri, P. (Eds.) *Methods in Applied Soil Microbiology and Biochemistry*; Academic Press: London, UK, 1995.
44. Wu, J.; Joergensen, R.G.; Pommerening, B.; Chaussod, R.; Brookes, P.C. Measurement of soil microbial biomass C by fumigation-extraction—An automated procedure. *Soil Biol. Biochem.* **1990**, *22*, 1167–1169. https://doi.org/10.1016/0038-0717(90)90046-3.
45. Brookes, P.C.; Landman, A.; Pruden, G.; Jenkinson, D.S. Chloroform fumigation and the release of soil nitrogen: A rapid direct extraction method to measure microbial biomass nitrogen in soil. *Soil Biol. Biochem.* **1985**, *17*, 837–842. https://doi.org/10.1016/0038-0717(85)90144-0.

46. Vance, E.D.; Brookes, P.C.; Jenkinson, D.S. An extraction method for measuring microbial biomass C. *Soil Biol. Biochem.* **1987**, *19*, 703–707. https://doi.org/10.1016/0038-0717(87)90052-6.
47. Anderson, T.H.; Domsch, K.H. The metabolic quotient for CO_2 (qCO_2) as a specific activity parameter to assess environmental effects on microbial biomass. *Soil Biol. Biochem.* **1993**, *25*, 393–395. https://doi.org/10.1016/0038-0717(93)90140-7.
48. Shi, S.; Kumar, S.; Young, S.; Maclean, P.; Jauregui, R. Evaluation of 16S rRNA gene primer pairs for bacterial community profiling in an across soil and ryegrass plant study. *J. Sustain. Agric. Environ.* **2023**, *2*, 500–512. https://doi.org/10.1002/sae2.12075.
49. White, T.J.; Bruns, T.; Lee, S.; Taylor, J. Amplification and direct sequencing of fungal ribosomal RNA genes for phylogenetics. In *PCR Protocols: A Guide to Methods and Applications*; Innis, M.A.; Gelfand, D.H.; Sninsky, J.J.; White, T.J., Eds.; Academic Press: San Diego, CA, USA, 1990; pp. 315–322. https://doi.org/10.1016/B978-0-12-372180-8.50042-1.
50. Rognes, T.; Flouri, T.; Nichols, B.; Quince, C.; Mahé, F. VSEARCH: A versatile open source tool for metagenomics. *PeerJ* **2016**, *4*, e2584. https://doi.org/10.7717/peerj.2584.
51. Edgar, R.C. UNOISE2: Improved error-correction for Illumina 16S and ITS amplicon sequencing. *bioRxiv* **2016**, 081257. https://doi.org/10.1101/081257.
52. Edgar, R.C. Search and clustering orders of magnitude faster than BLAST. *Bioinformatics* **2010**, *26*, 2460–2461. https://doi.org/10.1093/bioinformatics/btq461.
53. Edgar, R.C. SINTAX: A simple non-Bayesian taxonomy classifier for 16S and ITS sequences. *bioRxiv* **2016**, 074161. https://doi.org/10.1101/074161.
54. Quast, C.; Pruesse, E.; Yilmaz, P.; Gerken, J.; Schweer, T.; Yarza, P.; Peplies, J.; Glöckner, F.O. The SILVA ribosomal RNA gene database project: Improved data processing and web-based tools. *Nucleic Acids Res.* **2013**, *41*, D590–D596. https://doi.org/10.1093/nar/gks1219.
55. Nilsson, R.H.; Larsson, K.H.; Taylor, A.F.S.; Bengtsson-Palme, J.; Jeppesen, T.S.; Schigel, D.; Kennedy, P.; Picard, K.; Glöckner, F.O.; Tedersoo, L.; et al. The UNITE database for molecular identification of fungi: Handling dark taxa and parallel taxonomic classifications. *Nucleic Acids Res.* **2019**, *47*, D259–D264. https://doi.org/10.1093/nar/gky1022.
56. Katoh, K.; Standley, D.M. MAFFT multiple sequence alignment software version 7: Improvements in performance and usability. *Mol. Biol. Evol.* **2013**, *30*, 772–780. https://doi.org/10.1093/molbev/mst010.
57. Piñeiro, C.; Abuín, J.M.; Pichel, J.C. Very Fast Tree: Speeding up the estimation of phylogenies for large alignments through parallelization and vectorization strategies. *Bioinformatics* **2020**, *36*, 4658–4659. https://doi.org/10.1093/bioinformatics/btaa582.
58. Pinheiro, J.; Bates, D.; R Core Team. nlme: Linear and Nonlinear Mixed Effects Models; R package version 3.1-169, 2026. https://doi.org/10.32614/CRAN.package.nlme. Available online: https://CRAN.R-project.org/package=nlme (accessed on 22 October 2026).
59. Lenth, R.V. emmeans: Estimated Marginal Means, aka Least-Squares Means; R package version 2.0.3, 2026. https://doi.org/10.32614/CRAN.package.emmeans.
60. Benjamini, Y.; Hochberg, Y. Controlling the false discovery rate: A practical and powerful approach to multiple testing. *J. R. Stat. Soc. Ser. B* **1995**, *57*, 289–300. https://doi.org/10.1111/j.2517-6161.1995.tb02031.x.
61. Bray, J.R.; Curtis, J.T. An ordination of the upland forest communities of southern Wisconsin. *Ecol. Monogr.* **1957**, *27*, 325–349. https://doi.org/10.2307/1942268.
62. Anderson, M.J. A new method for non-parametric multivariate analysis of variance. *Austral Ecol.* **2001**, *26*, 32–46. https://doi.org/10.1111/j.1442-9993.2001.01070.pp.x.
63. Oksanen, J.; Simpson, G.L.; Blanchet, F.G.; Kindt, R.; Legendre, P.; Minchin, P.R.; O'Hara, R.B.; Solymos, P.; Stevens, M.H.H.; Szoecs, E.; et al. vegan: Community Ecology Package; R package version 2.7-5, 2026. https://doi.org/10.32614/CRAN.package.vegan. Available online: https://CRAN.R-project.org/package=vegan (accessed on 22 October 2026).
64. Anderson, M.J. Distance-based tests for homogeneity of multivariate dispersions. *Biometrics* **2006**, *62*, 245–253. https://doi.org/10.1111/j.1541-0420.2005.00440.x.
65. Levins, R. *Evolution in Changing Environments: Some Theoretical Explorations*; Princeton University Press: Princeton, NJ, USA, 1968. https://doi.org/10.2307/j.ctvx5wbbh.
66. Legendre, P.; Anderson, M.J. Distance-based redundancy analysis: Testing multispecies responses in multifactorial ecological experiments. *Ecol. Monogr.* **1999**, *69*, 1–24. https://doi.org/10.1890/0012-9615(1999)069[0001:DBRATM]2.0.CO;2.
67. R Core Team. *R: A Language and Environment for Statistical Computing*; R Foundation for Statistical Computing: Vienna, Austria, 2026. Available online: https://www.R-project.org/ (accessed on 22 October 2026).

68. Simpson, G.L. permute: Functions for Generating Restricted Permutations of Data; R package version 0.9-10, 2026. https://doi.org/10.32614/CRAN.package.permute. Available online: https://CRAN.R-project.org/package=permute (accessed on 22 October 2026).
69. Han, Q.; Fu, Y.; Qiu, R.; Ning, H.; Liu, H.; Li, C.; Gao, Y. Carbon amendments shape the bacterial community structure in salinized farmland soil. *Microbiol. Spectr.* **2023**, *11*, e0101222. https://doi.org/10.1128/spectrum.01012-22.
70. Wang, Y.; Tian, G.; Zhao, Q.; Li, D.; He, S. Temporal dynamics and optimal dose effects of biochar on soil properties, cotton growth, and bacterial community assembly in saline-alkali soils. *BMC Plant Biol.* **2025**, *25*, 1337. https://doi.org/10.1186/s12870-025-07415-8.
71. Stegen, J.C.; Lin, X.; Fredrickson, J.K.; Chen, X.; Kennedy, D.W.; Murray, C.J.; Rockhold, M.L.; Konopka, A. Quantifying community assembly processes and identifying features that impose them. *ISME J.* **2013**, *7*, 2069–2079. https://doi.org/10.1038/ismej.2013.93.
72. Ning, D.; Yuan, M.; Wu, L.; Zhang, Y.; Guo, X.; Zhou, X.; Yang, Y.; Arkin, A.P.; Firestone, M.K.; Zhou, J. A quantitative framework reveals ecological drivers of grassland microbial community assembly in response to warming. *Nat. Commun.* **2020**, *11*, 4717. https://doi.org/10.1038/s41467-020-18560-z.
73. Li, C.; Jin, L.; Zhang, C.; Li, S.; Zhou, T.; Hua, Z.; Wang, L.; Ji, S.; Wang, Y.; Gan, Y.; Liu, J. Destabilized microbial networks with distinct performances of abundant and rare biospheres in maintaining networks under increasing salinity stress. *iMeta* **2023**, *2*, e79. https://doi.org/10.1002/imt2.79.
74. ASTM. ASTM D1762-84: Standard Test Method for Chemical Analysis of Wood Charcoal. 1984.

Disclaimer/Publisher's Note: The statements, opinions and data contained in all publications are solely those of the individual author(s) and contributor(s) and not of MDPI and/or the editor(s). MDPI and/or the editor(s) disclaim responsibility for any injury to people or property resulting from any ideas, methods, instructions or products referred to in the content.